Published: 21st November 2025

ANACHEM JOURNAL
ISSN: 2006-5221 (Online)

MACHINE LEARNING ASSISTED MODELLING OF CHEMICALLY FUNCTIONALIZED NANOTUBES: A COMPUTATIONAL STUDY FOR THE ADSORPTION OF HYDROCARBON PETROLEUM POLLUTANTS

*[1]Hitler, L, Egbuchunam, T. O and Mbonu, I. J.

[1]Department of Chemistry, College of Science, Federal University of Petroleum Resources, Effurun, Nigeria.

***Corresponding author's email:** louismuzong@gmail.com

DOI:10.5281/zenodo.17622939

ABSTRACT

The potential of the newly modelled chemically functionalized nanotubes, Fe-Se@SiCNT, Os-Se@SiCNT, and Ru-Se@SiCNT materials, was studied based on a theoretical calculation scheme using density functional theory (DFT) for the remediation of butane (BTN), cyclopentane (CPN), and methylpropane (MPN) petroleum pollutants. The chemisorption phenomenon was observed for all configurations, with the Fe-Se@SiCNT material exhibiting the highest adsorption energy (Eads) towards gas adsorption. The adsorption energy (E_{ads}) of -0.640, -0.544, and -0.568 eV for the adsorption of BTN, CPN, and MPN pollutants, respectively, was obtained. The small energy gap of 1.042, 0.776, and 0.743 eV attributed to Fe-Se@SiCNT, Os-Se@SiCNT, and Ru-Se@SiCNT functionalized materials, respectively, significantly increased upon adsorption, showing good conductivity. A machine learning analysis was conducted to assess the predictive capabilities of four regression models (Linear Regression, Lasso Regression, Ridge Regression, and ElasticNet Regression) in predicting the Eads values obtained from the DFT-based analysis. All the models performed very well, with R^2 values ranging from 0.84 to 0.87 and root mean square errors (RMSEs) of 0.185 to 0.186. Among the four evaluated models, the ElasticNet Regression model forecasted the E_{ads} calculated through the DFT with the highest level of accuracy, with an R^2 of 0.8737, implying that it was able to better predict the variation in the adsorption energy data.

Keywords: Adsorption, nanotubes, hydrocarbon petroleum, DFT, machine learning

1.0. INTRODUCTION

Environmental pollution has increased rapidly in areas where petroleum-based facilities are located, primarily for the purpose of refining petroleum, diesel, kerosene, liquefied petroleum gas, and lubricating oil for human use (Pal and Sen, 2024). These toxic chemicals have had a severe effect on the health of human beings, making it critical and life-threatening. Although exposure to these pollutants may occur through breathing, touching, and consuming contaminated water and food, the most frequent route is inhalation of polluted air, which frequently causes both short-term and long-term disorders (Priyadarshanee *et al*., 2024). Nanomaterials have emerged as promising materials that could be utilized as sensors for the monitoring, adsorption, and evaluation of these pollutants (Zhang *et al*., 2019). Hence, this research focuses on the development of silicon-based nanotubes for the remediation of petroleum pollutants. In the current research, Selenium-doped silicon nanotubes (Se@SiCNT) are used as the starting material, which may be co-doped with iron-group (Fe, Ru, Os) transition metals to tune the electronic behaviour of the nanotubes, making them suitable for gas adsorption (Meshginqalam and Alaei, 2018).

In their work, Rezaie *et al.,* (2021) apply first-principles DFT calculations for the adsorption and detection of oil-dissolved gases, including hydrogen, ethylene, and methane, using ZnO-based nanomaterials. Similarly, Ajeel *et al.,* (2019) investigated some toxic associated petroleum gases using single-walled carbon nanotube (SWCNT) by applying the DFT/B3LYP calculations. Additionally, Okon *et al*., (2025) used some high-level theoretical calculations to investigate the adsorption and sensing mechanism of naphthalene-based polyaromatic hydrocarbon. Additionally, the theoretical interactions of transition metal-decorated carbon nanotubes with toluene, a petroleum-based pollutant, as a biosensor for the early diagnosis of cancer, have been investigated by Aasi *et al.,* (2020). Furthermore, and very recently, Mbonu *et al*., (2025) investigated some nanotubes and their transition metal derivatives as effective adsorbent materials for fuel oil desulfurization. In continuation of these research for the remediation of petroleum-based pollutants, herein, we are focusing on the adsorption and sensor properties of some very volatile petroleum products, particularly of linear alkanes such as butane (BTN), cyclic alkanes such as cyclopentane

(CPN), and the branched alkanes such as methylpropane (MPN) through the use of selenium and iron-group (Fe, Ru, Os) transition metal co-doping of silicon nanotube (SiCNT) as adsorbent materials.

2.0. COMPUTATIONAL DETAILS

2.1. Density functional theory (DFT) methods

The Density Functional Theory (DFT) framework was applied in the computational study, utilising the Gaussian16 software package (Frisch *et al*., 2016). It was based on generalised gradient approximation with Minnesota Hybrid Functional (M06-2X), along with the Def2-SVP basis set, which was adopted as our theoretical method. Optimisation of the Se-doped SiCNT surface was carried out, followed by substitution of the atoms by Fe, Os, and Ru to create the co-doped structures. The calculation of adsorption energies (E_{ads}) was done in the following expression:

$$E_{ads} = E_{complex} - E_{surface} - E_{adsobate}$$

Where the $E_{complex}$, $E_{surface}$, and $E_{adsorbate}$ represent the optimized energies of the complex, which is the pollutant and the surface together, the energy of the surfaces alone, and the energy of the adsorbate, respectively, as considered in the present study (Mbonu *et al*., 2025). HOMO-LUMO gap and NBO charge with dopant type, which helps predict and compare the sensing performance of Fe-, Os-, and Ru co-doped Se-doped SiCNT surfaces.

2.2. Machine learning design

In this work, four regression algorithms (Linear Regression, Ridge Regression, Lasso Regression, and Elastic Net Regression) were employed to accurately predict the adsorption energies of the biochar samples using a quantum chemical descriptor set for the dataset used to model the adsorption energies (Egemonye and Unimuke, 2024). These four regression algorithms were selected because each can produce accurate predictions with smaller amounts of data and is less prone to being overly fit by the data than other regression algorithms. Therefore, the relatively small dataset obtained from theoretical studies, which contained columns for the HOMO, LUMO, energy gap, and adsorption energies of chemically activated pristine biochar materials, was used to generate the machine learning predictions. A detailed description of the regression models used to make the machine-learning predictions will be provided in the subsequent sections.

3.0. Results and Discussion

3.1 Geometry optimization

The study of structural geometry involves the geometry of atoms, molecules, and other chemical species within a material or compound (Okon *et al*., 2025). The optimization of geometry led to the identification of several essential bonds, which showed the character of the interactions of the doped surface with the adsorbate, as shown in **Figure 1**. The Si-C bond (1.78-1.85 Å) was in the normal covalent range and proved the stability of the Si-C framework. The Ru-C (1.952 Å) and Fe-C (1.991 Å) bonds were short enough to suggest the strong interaction of metals with carbon, which was the chemisorption and potential charge transfer between the metal site and the carbon surface (Egemonye *et al*., 2024). The adsorbate separations of 2.25 to 3.15 Å indicate weaker physisorption that is governed by van der Waals forces. In the meantime, intermolecular C-C and C=C bonds (1.33-1.79 Å) were hardly changed, which indicated that the adsorbate structure did not change significantly during adsorption. Nevertheless, chemisorption is confirmed by the shorter metal-carbon bond. In contrast, the greater distance to the surface indicates physical adsorption, which suggests that the optimal geometry has achieved a stable and beneficial structure.

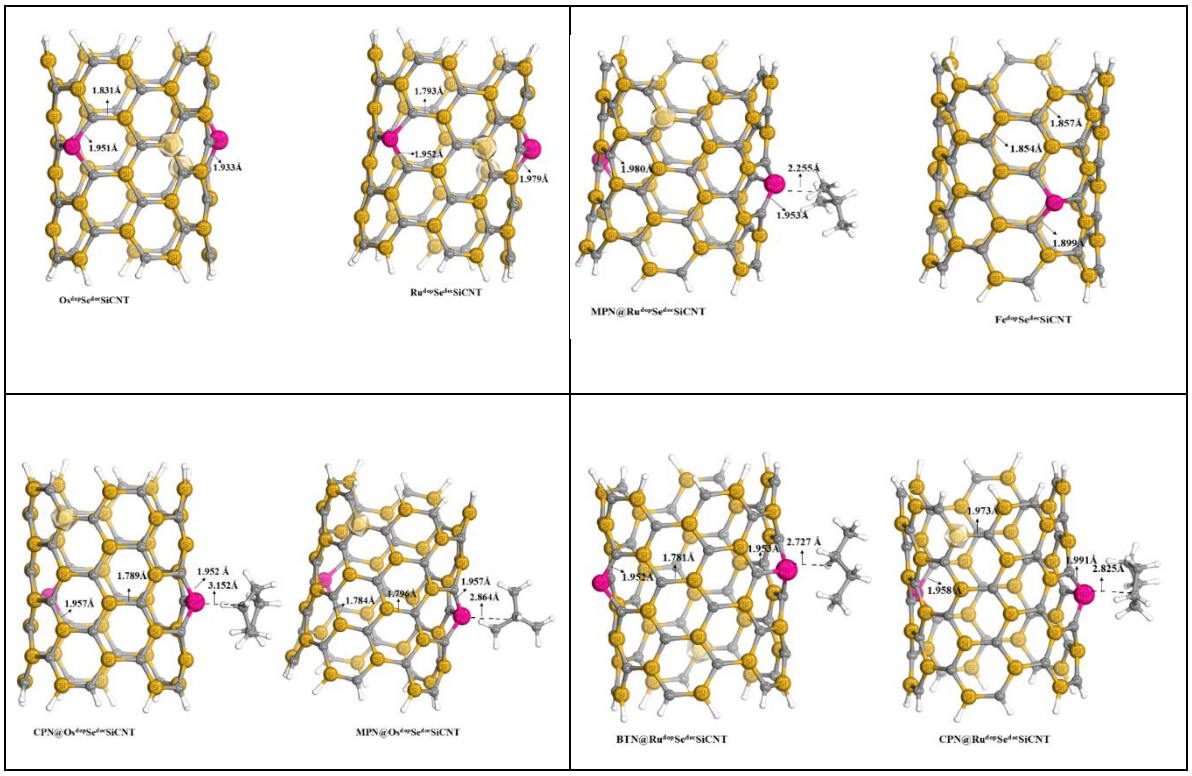

Figure 1. Geometry studies for the modelled systems

3.2. Electronic property studies

3.2.1 HOMO-LUMO and Quantum Descriptors

DFT/MN12SX/LANL2DZ computational methods were used to study the electronic properties of the systems under study, and the summarized results are shown in **Table 1.0** and **Figures 2(a) – (d)**. The HOMO and LUMO energies represent donating and accepting capabilities of electrons, respectively, whereas the energy gap represents stability and chemical reactivity (Louis *et al*., 2023). The value of Egap in (SiCNT) is 2.432 eV, which is highly stable with low reactivity. Fe, Os, and Ru doping led to a sizeable decrease in the size of the energy gap to 1.042 eV, 0.776 eV, and 0.743 eV, respectively, indicating a lower barrier to charge transfer and increased chemical reactivity. The lower Egap of Ru@SiCNT confirms its superior adsorption and catalytic potential. Doping reduced the gap to 1.042 eV (Fe@SiCNT), 0.776 eV (Os@SiCNT), and 0.743 eV (Ru@SiCNT), showing that Ru@SiCNT is the most reactive and best for charge transfer. Its ionization potential (IP) of 4.703 eV and electron affinity (EA) of 3.960 eV reflect a strong electron-accepting ability. The chemical potential (4.332 eV) and low hardness (0.372 eV) signify high softness and easy polarization (1.346). The electrophilicity (25.252 eV) is also highest for Ru@SiCNT, confirming its superior adsorption and reactivity compared to the pristine and other doped systems (Parker *et al*., 2025).

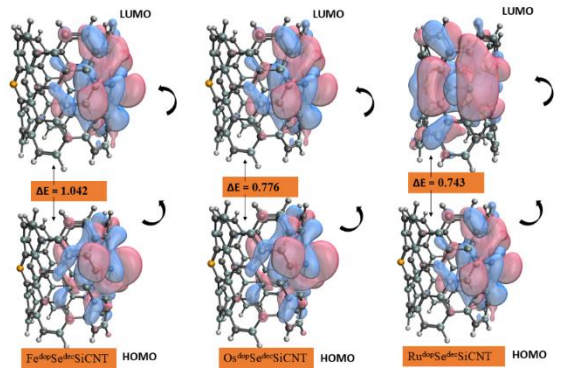

Figure 2 (a). Graphical illustration of the respective HOMO to LUMO transitions and localization of orbitals for the studied surfaces

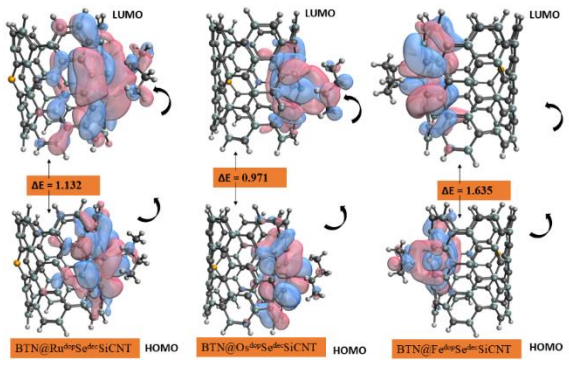

Figure 2 (b). Graphical illustration of the respective HOMO to LUMO transitions and localization of orbitals for the BTN interactions.

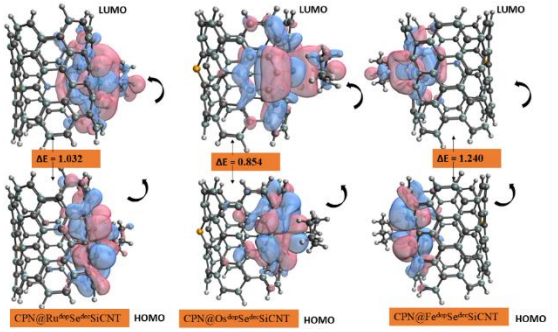

Figure 2 (C). Graphical illustration of the respective HOMO to LUMO transitions and localization of orbitals for the CPN interactions.

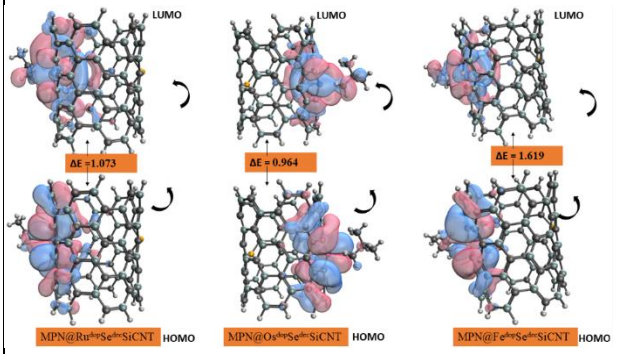

Figure 2 (d). Graphical illustration of the respective HOMO to LUMO transitions and localization of orbitals for the MPN interactions.

Table 1. Summary of the HOMO-LUMO energy gap and chemical quantum descriptors based on Koopman's approximations, calculated at DFT/MN12SX/LANL2DZ computational method.

Systems	E_{HOMO}	E_{LUMO}	E_{Gap}	IP	EA	μ	η	S	ω	N_{max}
Se@SiCNT	-5.070	-2.638	2.432	5.070	2.638	3.854	1.216	0.411	6.107	-3.169
Fe-Se@SiCNT	-4.960	-3.917	1.042	4.960	3.917	4.438	0.521	0.959	18.896	-8.515
Os-Se@SiCNT	-4.448	-3.672	0.776	4.448	3.672	4.060	0.388	1.289	21.251	-10.468
Ru-Se@SiCNT	-4.703	-3.960	0.743	4.703	3.960	4.332	0.372	1.346	25.252	-11.658
BTN-Fe-Se@SiCNT	-4.886	-3.250	1.635	4.886	3.250	4.068	0.818	0.612	10.121	-4.976
BTN-Os-Se@SiCNT	-4.422	-3.451	0.971	4.422	3.451	3.937	0.485	1.030	15.965	-8.111
BTN-Ru-Se@SiCNT	-4.655	-3.523	1.132	4.655	3.523	4.089	0.566	0.883	14.767	-7.224
CPN-Fe-Se@SiCNT	-4.887	-3.647	1.240	4.887	3.647	4.267	0.620	0.807	14.688	-6.884
CPN-Os-Se@SiCNT	-4.377	-3.523	0.854	4.377	3.523	3.950	0.427	1.171	18.270	-9.250
CPN-Ru-Se@SiCNT	-4.640	-3.609	1.032	4.640	3.609	4.125	0.516	0.969	16.491	-7.997
MPN-Fe-Se@SiCNT	-4.895	-3.276	1.619	4.895	3.276	4.086	0.810	0.618	10.309	-5.047
MPN-Os-Se@SiCNT	-4.427	-3.463	0.964	4.427	3.463	3.945	0.482	1.037	16.139	-8.182
MPN-Ru-Se@SiCNT	-4.659	-3.586	1.073	4.659	3.586	4.123	0.536	0.932	15.844	-7.686

Note: All units are in electron Volt (eV), except for S with a unit of eV^{-1}. N_{max} is dimensionless.

3.2.2 Natural bond orbital (NBO) analysis

The NBO results in **Table 2.0** show the donor-acceptor interactions responsible for charge transfer and molecular stability (Okon *et al.*, 2025). The stabilization energy E(2) reflects the strength of electron delocalization between donor and acceptor orbitals- higher E(2) values indicate stronger interactions. Se@SiCNT exhibits the highest E(2) of 1.473.44 kcal/mol, confirming strong internal charge delocalization and structural stability. After doping, the values decrease slightly at Fe-Se@SiCNT (721.54 kcal/mol), Os-Se@SiCNT (826.94 kcal/mol), and Ru-Se@SiCNT (561.92 kcal/mol), showing redistribution of charge toward the metal sites. Among the complexes, MPN-Ru-Se@SiCNT and BTN-Fe-Se@SiCNT exhibit relatively high stabilization energies

(1466.30 and 6.40.89 kcal/mol), indicating strong donor-acceptor coupling. Hence, the NBO data confirms effective charge transfer between the adsorbate and the doped surface, enhancing adsorption and chemical reactivity (Louis *et al*., 2023).

Table 2. Summary of the NBO analysis result calculated at DFT/MN12SX/LANL2DZ/Auto computational method.

Complexes	**Donor**	**Acceptor**	**E(2)/Kcalmol^{-1}**	**E(i)-E(j)/a.u**	**F(i,j)/a.u**
Se@SiCNT	LPC_{34}	$\pi^*(C_{39} - Se_{100})$	1473.44	0.09	0.327
Fe-Se@SiCNT	$\pi(C_{27} - Si_{62})$	$\pi^*(C_{59} - Si_{97})$	721.54	0.02	0.117
Os-Se@SiCNT	σ^*C_{58}	$\pi^*(C_{58} - Os_{100})$	826.94	1.13	0.896
Ru-Se@SiCNT	$\sigma^*(C_{27} - Si_{92})$	$\pi^*(C_{27} - Ru_{100})$	561.22	0.71	0.601
BTN-Fe-Se@SiCNT	$\sigma^*(C_{50} - Fe_{100})$	$\sigma^*(C_{27} - Fe_{100})$	640.89	0.07	0.400
BTN-Os-Se@SiCNT	$\sigma^*(C_{27} - Os_{100})$	$\sigma^*(C_{24} - Os_{100})$	253.75	0.04	0.213
BTN-Ru-Se@SiCNT	$\sigma^*(C_{27} - Ru_{100})$	$\sigma^*(C_{24} - Ru_{100})$	739.87	0.03	0.328
CPN-Fe-Se@SiCNT	$\sigma^*(C_{27} - Fe_{100})$	$\sigma^*(C_{24} - Fe_{100})$	1000.55	0.01	0.276
CPN-Os-Se@SiCNT	$\sigma^*(C_{24} - Os_{100})$	LP^*Os_{100}	826.67	0.01	0.192
CPN-Ru-Se@SiCNT	$\sigma^*(C_{27} - Ru_{100})$	$\sigma^*(C_{24} - Ru_{100})$	506.78	0.02	0.193
MPN-Fe-Se@SiCNT	$\sigma^*(C_{27} - Fe_{100})$	$\sigma^*(C_{24} - Fe_{100})$	1466.30	0.02	0.373
MPN-Os-Se@SiCNT	$\sigma^*(C_{58} - Os_{100})$	$\sigma^*(C_{47} - Os_{100})$	224.65	0.05	0.204
MPN-Ru-Se@SiCNT	$\sigma^*(C_{58} - Ru_{100})$	$\sigma^*(C_{27} - Ru_{100})$	291.86	0.06	0.252

3.3 Adsorption studies

The adsorption energy results in **Table 3.0** reveal the interaction strength and stability of BTN, CPN, and MPN molecules on Fe-, Os-, and Ru- co-doped Se@SiCNT surfaces (Mbonu *et al*., 2020). Adsorption energies (Eads) are all negative, confirming spontaneous and exothermic interactions. Among them, BTN-Fe-Se@SiCNT shows the most negative value (-14.764 kcal/mol), indicating the strongest adsorption and highest surface reactivity. Comparatively, MPN-Os-Se@SiCNT (-13.107 kcal/mol) and CPN-Fe-Se@SiCNT (-10.584 kcal/mol) also exhibit considerable interaction, while MPN-Ru-Se@SiCNT (-9.632 kcal/mol) shows relatively weaker adsorption. The variation in adsorption strength suggests that Fe doping enhances charge transfer and bonding more effectively than Os and Ru (Zhu *et al*., 2022). The overall results indicate that Fe-doping in SiCNT provides the most stable adsorption site for hydrocarbon attachment, which can be useful for sensing applications.

Table 3.0. Summarized adsorption energy results in Hartree, eV, and Kcal/mol calculated at DFT/MN12SX/LANL2DZ/Auto computational method

Complexes	$E_{Complex}$	$E_{Surface}$	$E_{Pollutants}$	Eads/Hartree	Eads/eV	Eads/Kcal/mol
BTN-Fe-Se@SiCNT	-1971.063218	-1812.775158	-158.264532	-0.024	-0.640	-14.764
BTN-Os-Se@SiCNT	-1939.301236	-1781.026658	-158.264532	-0.010	-0.273	-6.304
BTN-Ru-Se@SiCNT	-1942.060386	-1783.778787	-158.264532	-0.017	-0.464	-10.710
CPN-Fe-Se@SiCNT	-2009.131772	-1812.775158	-196.336626	-0.020	-0.544	-12.543
CPN-Os-Se@SiCNT	-1977.371344	-1781.026658	-196.336626	-0.008	-0.219	-5.058
CPN-Ru-Se@SiCNT	-1980.132608	-1783.778787	-196.336626	-0.017	-0.468	-10.790
MPN-Fe-Se@SiCNT	-1971.062443	-1812.775158	-158.266397	-0.021	-0.568	-13.107
MPN-Os-Se@SiCNT	-1939.300453	-1781.026658	-158.266397	-0.007	-0.201	-4.642
MPN-Ru-Se@SiCNT	-1942.060534	-1783.778787	-158.266397	-0.015	-0.418	-9.632

3.4 DFT adsorption energies (*Eads*) and Machine learning (ML)

The work presented here is the result of the combination of DFT results and Machine Learning (ML) models to determine adsorption energy (Eads) values for different VOCs using several functionalized surfaces; specifically, three metal functionalized surfaces (Fe, Os, and Ru) were examined in relation to butane (BTN), cyclopentane (CPN), and methylpropane (MPN) as shown in **Figure 3**. The DFT calculations provided the Eads values used as target values to train and evaluate the ML regression models, offering a significantly faster method for predicting adsorption properties. Results from the DFT model indicated that the functionalized surface made with iron (Fe) consistently achieved the highest adsorption energies for all the VOCs studied. For example, the adsorption energy value for BTN-Fe-Se@SiCNT was −0.64 eV, the adsorption energy value for CPN-Fe-Se@SiCNT was −0.544 eV, and the adsorption energy value for MPN-Fe-Se@SiCNT was −0.568 eV.

In contrast, the functionalized surface made with osmium (Os) demonstrated the least amount of adsorption among all the VOCs studied, with adsorption energy values such as −0.273 eV for BTN-Os-Se@SiCNT and −0.219 eV for CPN-Os-Se@SiCNT. The ruthenium (Ru) prepared surface exhibited an intermediate degree of adsorption strength and thus, not as good as those prepared with iron (Fe), but better than those prepared with osmium (Os). These tendencies indicate that the most favorable alternative for the adsorption of VOCs on the iron (Fe)-functionalized surfaces is their adsorption properties. A machine learning analysis was conducted to assess the predictive capabilities of the four regression models (Linear Regression, Lasso Regression, Ridge Regression, and

ElasticNet Regression) in predicting the Eads values obtained from the DFT-based analysis. All the models were very good with R^2 value of 0.84 to 0.87 and a root mean square error (RMSE) of 0.185 to 0.186. Among the four evaluated models, the ElasticNet Regression model forecasted the Eads calculated through the DFT with the highest level of accuracy, with an R^2 of 0.8737, implying that it was able to better predict the variation in the adsorption energy data. Hence, the joint use of DFT and machine learning models is an efficient method of speeding up the discovery and optimization of new materials (Egemonye and Unimuke, 2024). Fe-functionalized interfaces thus appear to be the optimal option for VOC adsorption, as indicated by DFT and machine learning algorithms, particularly ElasticNet Regression, which demonstrates remarkable predictive performance. Such a combined method will enable the rapid identification and design of highly effective adsorbing materials, providing some advantages both industrially and environmentally.

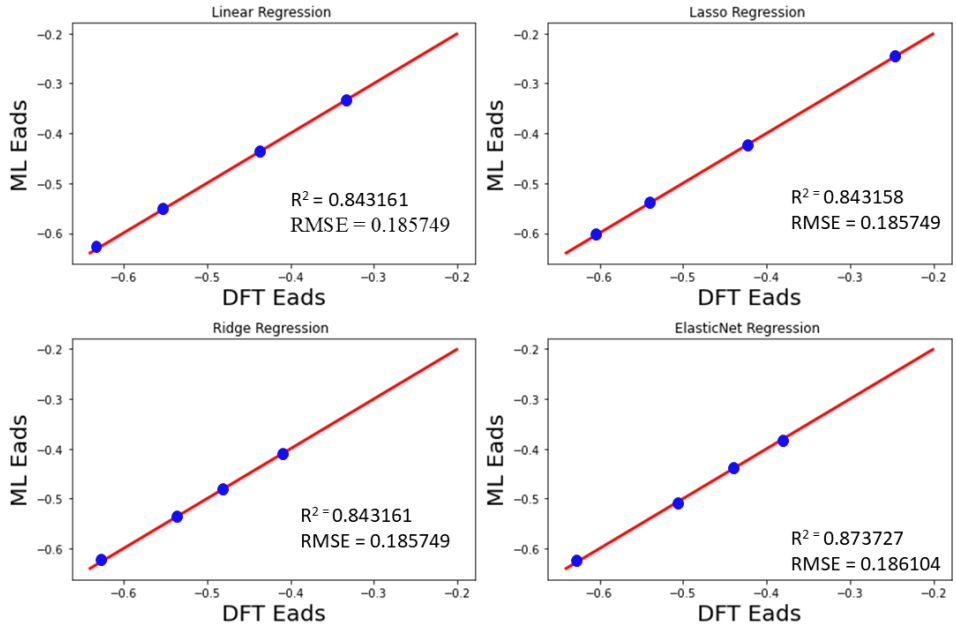

Figure 3. Comparison of DFT adsorption energies (Eads) with machine learning (ML) prediction Linear Regression, Lasso Regression, Ridge Regression, and ElasticNet Regression prediction models. The high correlation ($R^2 > 0.84$) and low RMSE values (approximately 0.185) across all models confirm the accuracy of ML in forecasting Eads values, with elastic Net regression achieving the highest accuracy ($R^2 = 0.8737$).

4.0. CONCLUSIONS

The computational analysis investigated the structural, electronic, and adsorption properties of pristine and metal-doped SiCNT (Fe, Os, and Ru) surfaces in interaction with three hydrocarbon molecules (BTN, CPN, and MPN) using DFT/MN12SX/LANL2DZ methods of surface analysis. Optimization of geometry indicates that metal doping causes a significant decrease in the energy gap and a better charge distribution, which proves the

enhanced chemical reactivity. The existence of highly Si-C, Fe-C, Os-C, and Ru-C bonds denotes that the dopant and the SiCNT surface are in a stable coordination state and high orbital overlap. Natural Bond Orbital (NBO) analysis also indicates that there is a large amount of charge transfer between donor and acceptor orbitals, indicating the presence of a greater electronic delocalization and bonding strength. Fe-doped Se@SiCNT has the largest stabilization energy of all of the systems, which is indicative of stronger orbital interactions.

Adsorption energy analysis indicates that the doped surfaces are biased towards negative values of adsorption, which suggests spontaneous and stable adsorption processes. Notably, BTN-Fe-Se@SiCNT exhibits the lowest adsorption energy, indicating that it is the most effective adsorbate. Fe-doped Se@SiCNT has greater reactivity, electronic stability, and adsorption behaviour; thus, it is a highly promising sensor and environmental remediation candidate. As such, combining DFT and machine learning models is an effective method of discovering and optimizing new materials faster. Thus, Fe-functionalized surfaces can be considered the best option for VOC adsorption, as demonstrated by the results obtained using DFT and machine learning models, specifically ElasticNet Regression, which exhibit the highest prediction potential. Such a combined method enables the quick selection and design of beneficial adsorbing materials and could provide numerous benefits in both industrial use and environmental contexts.

Acknowledgment

The authors are thankful to the Centre for High Performance Computing, South Africa, for the computational resources.

References

Ajeel, F. N., Mohammed, M. H., & Khudhair, A. M. (2019). SWCNT as a model nanosensor for associated petroleum gas molecules: via DFT/B3LYP investigations. *Russian Journal of Physical Chemistry B*, *13*(1), 196-204.

Aasi, A., Aghaei, S. M., & Panchapakesan, B. (2020). A density functional theory study on the interaction of toluene with transition metal decorated carbon nanotubes: a promising platform for early detection of lung cancer from human breath. *Nanotechnology*, *31*(41), 415707.

Egemonye, T. C., & Unimuke, T. O. (2024). Machine learning-assisted DFT-prediction of pristine and endohedral doped (O and Se) Ge12C12 and Si12C12 nanostructures as anode materials for lithium-ion batteries. *Scientific Reports*, *14*(1), 26244.

Frisch, M. E., Trucks, G. W., Schlegel, H. B., Scuseria, G. E., Robb, M., Cheeseman, J. R., ... & Fox, D. J. (2016). Gaussian 16.

Louis, H., Chukwuemeka, K., Agwamba, E. C., Abdullah, H. Y., & Pembere, A. M. (2023). Molecular simulation of Cu, Ag,

and Au-decorated Si-doped graphene quantum dots (Si@ QD) nanostructured as sensors for SO_2 trapping. *Journal of Molecular Graphics and Modelling*, *124*, 108551.

Meshginqalam, B., & Alaei, S. (2018). Transition metals adsorption and conductivity modification in carbon nanotubes: analytical modeling and DFT study. *Adsorption*, *24*(6), 575-583.

Mbonu, I. J., Udowa, E. O., Okhuarobo, O. J., Odey, S. E., & Runde, M. (2025). Insight into the chemical tailoring of nanotube and its metal-doped derivatives for fuel oil desulfurization: First-principles studies. *Journal of the Indian Chemical Society*, 101876.

Okon, E. O., Mathias, G. E., Runde, M., Abed, M. A. K., & Pathmanathan, K. (2025). Adsorption of polycyclic aromatic hydrocarbon (PAH): A computational study of naphthalene interactions with chemically functionalized nanotubes. *Materials Science in Semiconductor Processing*, *194*, 109533.

Pal, D., & Sen, S. (2024). In-depth coverage of petroleum waste sources, characteristics, environmental impact, and sustainable remediation process. In *Impact of petroleum waste on environmental pollution and its sustainable management through circular economy* (pp. 1-38). Cham: Springer Nature Switzerland.

Priyadarshanee, M., Mahto, U., & Das, S. (2022). Mechanism of toxicity and adverse health effects of environmental pollutants. In *Microbial biodegradation and bioremediation* (pp. 33-53). Elsevier.

Parkar, P., Chaudhari, A., Sonawane, M. R., & Nagare, B. J. (2025). SO2 sensing performance of silicon substitutional doped (8, 0) carbon nanotube: A density functional theory study. *Talanta Open*, *11*, 100403.

Rezaie, S., Bafghi, Z. G., Manavizadeh, N., & Kordmahale, S. B. (2021). Highly sensitive detection of dissolved gases in transformer oil with carbon-doped ZnO nanotube: A DFT study. *IEEE Sensors Journal*, *22*(1), 82-89.

Zhang, Y. N., Niu, Q., Gu, X., Yang, N., & Zhao, G. (2019). Recent progress on carbon nanomaterials for the electrochemical detection and removal of environmental pollutants. *Nanoscale*, *11*(25), 11992-12014.

Zinouri, R., Romani, N. N., Gokeh, M. S., Vandani, S. A. K., Alipourfard, I., & Kadhim, M. M. (2022). DFT study on sensing properties of twisted nano graphene ($C_{80}H_{30}$) towards toxic sulfur gases (environmental pollution). *Chemical Physics*, *562*, 111624.

Zhu, Y., Li, X., Chen, P., & Zhu, B. (2022). Ru-doped magnetic nanoparticles embedded in mesoporous silica for effective microwave absorption by interface engineering and DFT calculations. *Microporous and Mesoporous Materials*, *333*, 111763.